

Periodic and High-Temperature Disordered Conformations of Polytetrafluoroethylene Chains: An *ab Initio* Modeling

Maddalena D'Amore, Giovanni Talarico, and Vincenzo Barone*

Contribution from the Dipartimento di Chimica, Università degli Studi di Napoli "Federico II", via Cintia, 80126 Napoli, Italy

Received May 17, 2005; E-mail: baronev@unina.it

Abstract: We report here the main results of a successful attempt to predict some macroscopic properties of representative polymers of technological relevance both in regular and disordered forms by using first principle quantum mechanical approaches at microscopic level. Until now, the prediction of the structural and thermal properties of those polymers has been mostly a domain of molecular mechanics methods. To overcome the limits of those classical computational tools whenever physical properties are significantly influenced by stereoelectronic effects (e.g., electron rich substituents), we employed methods rooted in the Density Functional Theory (DFT). A general computational strategy including the proper choice of periodic boundary conditions (PBC), functional, basis set, and model system size, has been tested and validated for saturated polymers such as polyethylene and isotactic/syndiotactic polypropylenes. On the basis of these results, a comprehensive study of poly(tetrafluoroethylene) (PTFE) chains in both regular periodic and disordered conformations has been performed. A statistical approach has been next applied to obtain the thermal concentration of defects and to reproduce the thermal behavior of the investigated polymer. At the end, a very good agreement with experimental X-ray diffraction and IR results has been achieved, definitely reaching a good understanding of the widely studied disorder phenomenon determining the main technological properties of poly(tetrafluoroethylene) (the trade Teflon) and, at the same time, identifying the proper computational tools to investigate perfluoro-compounds and other complex polymeric systems.

Introduction

Predicting the macroscopic properties of large complex systems using first principle quantum mechanical approaches at microscopic level can be considered in a sense the Holy Grail of theoretical and/or computational methods. The general path toward this objective starts from precise evaluation of structural and energetic parameters of big size systems which, introduced into statistic thermodynamic equations (or, more often, numerical simulations), lead to the macroscopic quantities to be directly compared with experiments. One of the most remarkable successes of computational chemistry is the realization of this project for the ground electronic state of small closed-shell systems not containing too heavy atoms in the gas phase. Unfortunately, the situation is much more involved for more complex systems.

For this reason, the structural characterization of large complex systems such as polymeric materials has been traditionally a "domain" of molecular mechanics methods,¹ with few recent attempts by semiempirical models, whereas the application of *ab initio* methods in this field is just beginning.^{2,3}

Thanks to recent computational developments, nowadays *ab initio* approaches might be of big help in elucidating many

physicochemical phenomena involving polymers. This is the case particularly whenever physical properties are influenced not only by steric but also by electronic effects such as electron-rich substituents, conjugated systems, the presence of aromatic groups, or in all cases where molecular mechanics and semiempirical methods fail. However, due to the size of the considered systems, use of *ab initio* calculations requires the development and tuning of effective and reliable computational strategies.

A paradigmatic example is represented by the complex polymorphic behavior of poly(tetrafluoroethylene) (PTFE), a polymer which exhibits peculiar mechanical properties that form the basis of its commercial use as Teflon. PTFE at atmospheric pressure shows a peculiar polymorphism involving three crystalline phases as the temperature increases.⁴ The three polymorphs are usually denoted as form II, stable at temperatures lower than 19 °C, form IV stable at temperatures between 19 and 30 °C, and form I stable at temperatures higher than 30 °C up to the melting point of 330 °C.⁴ At 19 °C form II transforms into form IV, which in turn transforms into form I at 30 °C, resulting in a steplike increase of disorder in the crystals.⁵

Form II has been described in terms of a close packing of helical chains containing 13 CF₂ units in 6 turns, the dihedral angles being only slightly distorted from the trans state (*T* =

(1) Leading reference: (a) Corradini, P.; Guerra, G. *Adv. Polym. Sci.* **1992**, *100*, 182. (b) De Rosa, C. *Top. Stereochem.* **2003**, *24*, 71 and references therein.

(2) Kudin, K.; Scuseria, G. E. *Phys. Rev. B* **2000**, *61*, 5141.

(3) Improta, R.; Kudin, K.; Scuseria, G. E.; Barone, V. *J. Am. Chem. Soc.* **2002**, *124*, 113.

(4) Sperati, C. A.; Starkweather, H. W., Jr. *Fortschr. Hochpolym. Forsch.* **1961**, *2*, 465.

(5) Pierce, R. H. H., Jr.; Clark, E. S.; Whitney, J. F.; Bryant, W. M. D. 130th Meeting of American Chemical Society, 1954, Atlantic City, NJ, p 9.

180°).⁶ Chains in a 13/6 conformation are packed in a nearly hexagonal lattice with $a' = b' = 5.59 \text{ \AA}$, $c = 16.9 \text{ \AA}$, $\gamma' = 119.3^\circ$.⁷ The 19 °C transition from form II to form IV corresponds to slight untwisting of helical chains, from 13/6 helix into 15/7 helix (15 CF₂ units in 7 turns).⁷ At the onset of phase transition, the molecular packing changes from an ordered triclinic structure into a disordered hexagonal structure with larger interchain distances. The chain repetition of PTFE in form IV corresponds to $c = 19.5 \text{ \AA}$, and at 20 °C, the chain axes are placed at the nodes of a hexagonal lattice with $a' = b' = 5.66 \text{ \AA}$. Extensive structural studies have indicated the presence in form IV of PTFE of a large amount of structural disorder, mainly related to the occurrence of small angular displacements of chains around their axes and of a slight translational disorder of chains parallel to their axes.⁸ At 30 °C form IV transforms into form I which is characterized by the presence of larger amounts of disorder; the chain conformation becomes more irregular, and long-range order is maintained only in the parallelism of chain axes and in their pseudo-hexagonal arrangement.⁵

The microscopic explanation of many properties of poly(tetrafluoroethylene) (in particular its high melting point) was found in the tendency of polymeric chains in form I to conformational disorder well below the above-reported melting point. The presence of this high entropic contribution already before melting, reducing the entropy difference in melting phenomenon, makes the melting point very high.

In these disordered conformations, ordered portions of chains in right- and left-handed 15/7 helical conformations succeed each other statistically along the chain. Evidences for the occurrence of helix reversal defects come from IR spectroscopic studies⁸ and X-ray diffraction experiments,^{9–12} which indicate that the concentration of helix reversal defects increases steeply with temperature in the intermediate form, between 19 and 30 °C, and levels off in the high temperature form as the temperature increases.¹²

Several studies based on molecular mechanics and ab initio conformational analyses (although employing the quite small perfluorobutane model) have been performed to reproduce the complex conformational behavior of poly(tetrafluoroethylene) with temperature.^{10,13–18} In some cases reasonable assumptions of a sequence of stems of different chirality connected by portions in transplanar conformation have been made to avoid the bowing of the chains. Unfortunately, from one side, these assumptions, inserting rigidity along the chains,^{10,16} are in contrast with the results of ab initio calculations for small perfluoro-*n*-alkanes (C₄F₁₀, C₅F₁₂), which predict minimum energy conformations with backbone dihedral angles shifted away from the trans position at 180°;^{13–15} on the other side,

the dimensions of the models used in ab initio studies are too small to be really representative of poly(tetrafluoroethylene) chains.^{13–15} At any rate, all these approaches did not reproduce correctly the conformational behavior of long chains of poly(tetrafluoroethylene) as the temperature increases. In fact, for the modeling of helix reversals in poly(tetrafluoroethylene) specific force fields have been developed,¹⁶ sometimes exploiting¹⁸ quantum mechanical studies of perfluorobutane to tune some parameters.

Molecular dynamics simulations (employing the latter force field)¹⁸ performed on realistic models of PTFE have been also exploited for the investigations of disorder in this complex system.

In none of the previous studies,^{16,18} minimum energy conformers have the right number of CF₂ groups per 180° turn (regular helix), or is the predicted temperature for the occurrence of the disordering transition in the range of experimental determinations. All the computed melting points are significantly far from the observed one, and the computed energies for a single helix reversal (defect) are not in agreement¹⁶ with the experimental one.⁸

In a previous paper¹⁹ we tried to study the disordered conformation of PTFE in the form I modeling defective conformations of PTFE chains containing helix reversals by the semiempirical PM3 approach.^{20,21} Our results indicate that straight and slim model chains of PTFE containing helix reversal defects may be obtained at a low cost of internal energy and with small lateral encumbrance without introducing at the junction between consecutive enantiomorphic portions of chains any dihedral angle in a trans conformation, as assumed in previous models.^{10,16,17} The presence of helix reversal defects induces a gradual coalescence of the diffuse scattering located on the seventh and eighth layer line (see next section), into a single diffraction halo centered between, as their concentration increases. According to PM3 computations, coalescence occurs when the helix reversal concentration reaches the critical value of ~ 1 inversion/16CF₂ units, which can be related, through a statistical model, to a critical value of the temperature. Thus, the PM3 approach has given some improvements in the understanding of disorder phenomena in PTFE: the way the reversals occur, the geometrical details of the junction between systems of different chirality, and so on. However, also this approach is not adequate from a quantitative point of view leading to an overestimation of the reversal cost and, consequently, of the critical temperature. In addition, the PM3 model does not predict fully reliable geometrical parameters.

Definitely, all the previous models reported in the literature^{9–19} do not reproduce the correct geometrical parameters and energetic defect contributions, the right helical structure for regular helices, and the disorder phenomena in poly(tetrafluoroethylene), suggesting to us that the theoretical prediction of PTFE properties can be considered until now an “unsuccessful story”.

Once identified precisely the limits of the previous computational approaches, to obtain an improved accuracy, which seems to be necessary to foresee the thermal behavior of PTFE

- (6) Bunn, C. W.; Howells, E. R. *Nature* **1954**, *174*, 549.
 (7) Clark, E. S.; Muus, L. T. Z. *Kristallogr.* **1962**, *117*, 119.
 (8) Brown, R. G. J. *Chem. Phys.* **1964**, *40*, 2900.
 (9) Corradini, P.; De Rosa, C.; Guerra, G.; Petraccone, V. *Macromolecules* **1987**, *20*, 3043.
 (10) Corradini, P.; Guerra, G. *Macromolecules* **1977**, *10*, 1410.
 (11) De Rosa, C.; Guerra, G.; Petraccone, V.; Centore, R.; Corradini, P. *Macromolecules* **1988**, *21*, 1174.
 (12) Kimmig, M.; Strobl, G.; Stühn, B. *Macromolecules* **1994**, *27*, 2481.
 (13) Dixon, D. A.; Van Catledge, F. A. *Int. J. Supercomput. Appl.* **1988**, *2*, 52.
 (14) Dixon, D. A. *J. Phys. Chem.* **1992**, *96*, 3698.
 (15) Rothlisberger, U.; Laasonen, K.; Klein, M. L.; Sprik, M. J. *Chem. Phys.* **1996**, *104*, 3692.
 (16) Holt, D. B.; Farmer, B. L. *Polymer* **1999**, *40*, 4667.
 (17) Holt, D. B.; Farmer, B. L. *Polymer* **1999**, *40*, 4673.
 (18) Sprik, M.; Rothlisberger, U.; Klein, M. J. *Phys. Chem. B* **1997**, *101*, 2745.

- (19) D'Amore, M.; Auriemma, F.; De Rosa, C.; Barone, V. *Macromolecules* **2004**, *37*, 9473.
 (20) Stewart, J. J. J. *J. Comput. Chem.* **1989**, *10*, 209.
 (21) Stewart, J. J. J. *J. Comput. Chem.* **1989**, *10*, 221.

and of its disordered form I, we resorted to methods rooted into the Density Functional Theory (DFT).^{22,23,24}

It is worth noting that the most direct way of examining electronic effects in an isolated chain of PTFE is to compute structures and energies of infinite chain models including all long-range interactions. For these reasons we decided to use, for the first time in this field, DFT methods based on localized functions and employing periodic boundary conditions (PBC)^{2,3} to regular forms of poly(tetrafluoroethylene), thus taking into the proper account long-range effects, which can often tune structural and energetic quantities.

First of all, the building blocks of a comprehensive computational approach consisting of a functional, basis set, number of *k* points, etc. have been validated on simpler polymer chains with special reference to the size of the model.

Since polyethylene (PE) and polypropylene (PP) are polymers whose crystal structures have been widely investigated and whose repetitive units have a relatively simple structure, we applied first the DFT/PBC methods to polyethylene with chains in a zigzag planar conformation (*t*PE), isotactic polypropylene in the helical conformation (*i*PP), and syndiotactic polypropylene with chains in *trans*-planar conformation (*s*PP)¹ by means of the conventional PBE functional.²⁵

The results prompted us to use the same computational tools to study the PTFE, whose conformational behavior and physical properties seem to be determined not only by steric effects but also by electronic ones. We started the analysis employing the same basis set and functional used for *n*-polyalkanes on perfluoro-oligomers of increasing length; then the study has been brought forward by extending the basis set and employing also a hybrid functional (PBE0).²⁶

To investigate disorder in high temperature form I of PTFE and to obtain relevant microscopic details, calculations have been performed on model chains of perfluoro-oligomers CF₃–(CF₂)_{*n*}–CF₃ of increasing length with different concentrations of defects.

Finally, once the most effective functional and basis set for perfluoro-compounds were identified, a refinement of the structure and energetics of conformational disorder in the high temperature form of poly(tetrafluoroethylene) has also been obtained by means of DFT calculations and the results elaborated with a statistical thermodynamic approach to predict the macroscopic properties of PTFE.

Quantum Mechanical Calculations. All calculations reported below have been performed by means of the Gaussian package.²⁷

We performed geometry optimizations on *t*PE, *i*PP, and *s*PP by means of the conventional PBE functional,²⁵ testing different basis sets and numbers of *k* points in order to reach an effective and accurate description of these systems.

In more detail, concerning *t*PE, geometry optimizations were performed using the conventional PBE functional and basis sets ranging from 6-31G(d) to 6-31+G(d,p), 6-311G(d,p)6d, and

6-311+G(d,p)6d;^{28,29} similarly, to obtain well converged energies and geometries for *t*PE, an increasing number of *k* points equal to 8, 16, 32, 64, 128, 200, and 400 has been considered. The repeating unit always consists of the (–CH₂–CH₂–) moiety.

For *i*PP the repeating unit consists of three monomeric (–CH₂CHCH₃–) units; the same basis sets and number of *k* points discussed above for *t*PE have been selected.

For *s*PP, a cell containing two monomeric units has been adopted; the starting point was a perfectly fully extended (*trans*) structure. Since the study of the previous two polymers has shown that diffuse functions do not influence the geometrical parameters, only calculations with 6-31G(d) and 6-311G(d,p) basis sets have been carried out.

As a starting point in the analysis of poly(tetrafluoroethylene), the C₂F₆, C₄F₁₀, C₅F₁₂, C₁₀F₂₂, and C₁₆F₃₄ oligomers of *n*-perfluoroalkanes have been considered. Geometry optimizations for these oligomers of increasing length have been carried out employing the conventional PBE and the hybrid PBE0 functionals, with 6-31G(d) and 6-31+G(d,p) basis sets.

Since DFT methods employing PBE, and especially the PBE0 functional, with the 6-31G(d) basis set reproduce the behavior of perfluoro-oligomers with remarkable accuracy, we applied to regular forms of poly(tetrafluoroethylene) the DFT methods with periodic boundary conditions (DFT/PBC). Starting from structures with 13 or 15 monomeric units per unit cell, the structures obtained from unconstrained optimizations of the helices and the stress tensor have been analyzed. Calculations have been carried out at PBE/6-31G(d) and PBE0/6-31G(d) levels.

It is worth recalling that PM3 calculations previously performed¹⁹ on oligomers with increasing numbers of monomeric units have shown that, starting from oligomers containing 16 CF₂ units, the geometry of the chain does not change significantly. Thus we performed *ab initio* calculations on oligomers of increasing size until 16 CF₂ units with reversals and without any reversal. Using the optimized structures with 16 monomeric units, larger oligomers of 60 CF₂ units have been built with different numbers of reversals.

As mentioned in the Introduction, the transition from form IV into form I has been characterized as a transition between a disordered state controlled by intra- and intermolecular forces into one which is only determined by intramolecular potentials.^{7,12} Most of the authors agree that in form I, at high temperature, any residual translational order parallel to chain axes and orientational order around chain axes are lost.^{7,9,12,30} For these reasons the Fourier transform of isolated chains may be advantageously compared to the diffracted intensity far from the equator, when there is a low degree of rotational (around the chain axis) and translational (along the chain axis) order between adjacent parallel chains.

As a consequence, calculations of Fourier transform on chain models obtained by means of *ab initio* computations have been performed to be compared with experimental X-ray diffraction patterns.

The X-ray diffraction profiles discussed in the following have been calculated as a function of the cylindrical coordinates ξ

(22) Hohenberg, P.; Kohn, W. *Phys. Rev.* **1964**, *136*, B864.
 (23) Parr, R. G.; Yang, W. *Density Functional Theory of atoms and molecules*; Oxford University Press: New York, 1989.
 (24) *Density Functional: theory and applications*, 500, *Lecture Notes in Physics*; Spiegel Verlag: Berlin, 1998.
 (25) Perdew, J. P.; Burke, K.; Ernzerhof, M. *Phys. Rev. Lett.* **1996**, *77*, 3685.
 (26) Adamo, C.; Barone, V. *J. Chem. Phys.* **1999**, *110*, 6158.
 (27) Frisch, M. J. et al. *Gaussian03*, release C.02; Gaussian Inc.: Pittsburgh, PA.

(28) Foresman, J. B.; Frisch, M. J. *Exploring Chemistry with Electronic Structure Methods*, 2nd ed.; Gaussian Inc.: Pittsburgh, PA, 1996.
 (29) Hariharan, P. C.; Pople, J. A. *Theor. Chim. Acta* **1973**, *23*, 213.
 (30) Yamamoto, T.; Hara, T. *Polymer* **1986**, *27*, 986.

Table 1. Geometrical Parameters for Minimum Energy Structures of *t*PE (a), *i*PP and *s*PP (b), Respectively^a

(a)	d_{c-c} (Å)	d_{c-H} (Å)	CCC (deg)	θ_1 (deg)	c (Å)				
<i>t</i> PE (k points = 64)									
PBE/6-31G(d)	1.535	1.109	113.6	180.0	2.570				
PBE/6-31+G(d,p)	1.536	1.108	113.7	180.0	2.573				
PBE/6-311G(d,p)6d	1.534	1.106	113.7	180.0	2.568				
PBE/6-311+G(d,p)6d	1.534	1.106	113.7	180.0	2.568				
(b)	d_{c-c} (Å)	d_{c-H} (Å)	d_{CCH_3} (Å)	$C_1C_2C_3$ (deg)	$C_2C_3C_4$ (deg)	CCCH ₃ (deg)	θ_1 (deg)	θ_2 (deg)	c (Å)
<i>i</i> PP									
PBE/6-31G(d)	1.546	1.109	1.538	117.5	111.3	109.4	-60.2	-179.3	6.558
(k points = 8)									
PBE/631+G(d,p)	1.546	1.108	1.539	117.6	111.4	109.4	-60.2	-179.3	6.566
(k points = 8)									
PBE/6-31+G(d,p)	1.545	1.108	1.539	117.6	111.4	109.4	-60.2	-179.3	6.566
(k points = 16)									
PBE/6-311G(d,p)6d	1.544	1.106	1.536	117.5	111.4	109.4	-60.1	-179.6	6.547
(k points = 8)									
PBE/6-311G(d,p)6d	1.542	1.106	1.536	117.5	111.4	109.4	-60.1	-179.6	6.547
(k points = 16)									
<i>s</i> PP (k points = 8)									
PBE/6-31G(d)	1.548	1.109	1.540	114.6	112.1	110.9	-162.6	162.6	5.137
PBE/6-311G(d,p)6d	1.546	1.106	1.538	114.6	112.1	110.9	-162.7	162.7	5.130

^a In particular, the torsion angles θ_1 and θ_2 (see Scheme 1) ($\theta_1 = \theta_2$ for *t*PE) and the valence angles (CCC for *t*PE, $C_1C_2C_3$ and $C_2C_3C_4$ for PP) along the chain are listed, and the period along the chain axis c is also reported. The structures have been obtained using a PBE functional with different basis sets; in the case of *i*PP, also results relative to a different numbers of k points have been reported.

and ζ , paying particular attention to the regions of reciprocal space corresponding to $\xi = 0 \text{ \AA}^{-1}$, $0.4 \text{ \AA}^{-1} < \zeta < 1 \text{ \AA}^{-1}$ (i.e., along the meridian) and for $\xi = 0.18 \text{ \AA}^{-1}$, $0.15 \text{ \AA}^{-1} < \zeta < 0.55 \text{ \AA}^{-1}$, because in these regions the experimental X-ray diffraction patterns of form I of PTFE show the most important information regarding the possible conformational disorder.

The square modulus of the structure factor (I_c), to be compared with the experimental X-ray fiber diffraction intensity (I), has been calculated using the following formula:

$$I_c = \sum_{ij} C_{ij} g_{ij} \quad (1)$$

The factors C_{ij} in eq 1 account for the interference between coupled atoms i and j

$$C_{ij} = f_i f_j J_0(2\pi\xi r_{ij}) \exp(2\pi\zeta z_{ij}) \quad (2)$$

and the second term (g_{ij}) accounts for the finite length of the chains:³¹

$$g_{ij} = (1 - 2p_c)^{|z_{ij}|/\Delta l} \quad (3)$$

In eq 1, the interference of atoms in 30 consecutive monomeric units in a chain (atomic coordinates x_i, y_i, z_i , atomic scattering factors f_i) with the remaining atoms along the chain (atomic coordinates x_j, y_j, z_j ; atomic scattering factors f_j) is considered. In eq 2 $r_{ij} = [(x_i - x_j)^2 + (y_i - y_j)^2]^{1/2}$ and z_{ij} ($= z_i - z_j$) are the distances in the xy plane and along z , respectively, between atoms i and j , and J_0 is the 0-th order Bessel function.³² In eq 3 Δl is the average axial advance per monomer, p_c represents a Bernoulli type probability that the chain ends up growing along the chain axis on each addition of a new CF_2 unit, and $\Delta l/p_c$ is the average correlation length of the chain.³³ In the calculations the value of $\Delta l/p_c$ has been fixed equal to

20 \AA , to reproduce the width at half-height of experimental diffraction peaks.

The average value of the diffraction intensity was calculated by choosing, for each reciprocal point (ξ, ζ), the reference sequence of 30 consecutive monomeric units at random, in the central region of the oligomer with $n = 60$, discarding the 3 terminal CF_2 units at both ends. This allows averaging the calculated intensity on conformers having different distributions of the length of the individual helical stems making the result of Fourier transform independent of the particular model of the conformation adopted in the calculations. We checked that, in the reciprocal space region of interest for our calculation, this method gave the same results when a classical averaging is instead performed, iterating the calculations of the Fourier transforms a number of times, each time choosing a different oligomer with a different distribution of length of individual helical portions and then averaging the so calculated intensities. This approach implies a short computation time and avoids the appearance in the calculated X-ray diffraction profiles of spurious maxima due to termination effects.

Results and Discussions

Modeling *n*-Polyalkane Chains. The structure predicted through DFT/PBC methods for *t*PE seems to be quite independent of the number of k points adopted, 8 k points providing essentially converged structures. The main geometrical parameters listed in Table 1a (Scheme 1) show that extension of the basis set to 6-31+G(d,p), 6-311G(d,p)6d, and 6-311+G(d,p)-6d has a negligible effect on the predicted geometrical parameters, which are, in turn, in good agreement with experiments.³⁴ The bond lengths and valence angles along the chain are well reproduced already at the 6-31G(d) level; in particular a very good agreement with experiment for the periodicity along the chain axis (c) has been found ($c = 2.5 \text{ \AA}$ according to X-ray diffraction).

(31) Auriemma, F.; Petraccone, V.; Parravicini, L.; Corradini, P. *Macromolecules* **1997**, *30*, 7554.

(32) Tadokoro, H. *Structure of Crystalline Polymers*; John Wiley & Sons: New York, 1979.

(33) (a) Allegra, G.; Bassi, I. *Gazz. Chim. Ital.* **1980**, *110*, 437. (b) Allegra, G.; Bassi, I.; Meille, V. *Acta Crystallogr.* **1978**, *A34*, 653.

(34) Bunn, W. *Trans. Faraday Soc.* **1939**, *35*, 482.

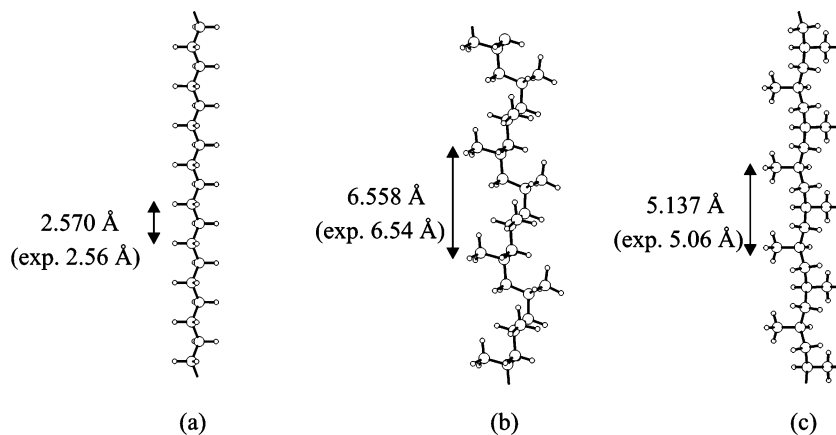
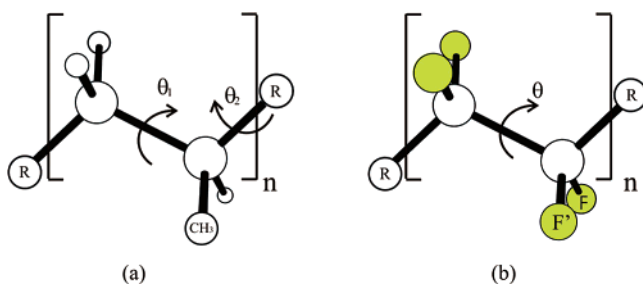


Figure 1. Regular helices predicted at the PBE/6-31G(d)/PBC level, for *t*PE (a), *i*PP (b), and *s*PP (c), respectively; their periods along the chain axis (in Å) are also reported.

Scheme 1



For *i*PP the number of k points does not significantly affect the geometry of the chain as one can see from the results reported (for some basis sets) in Table 1b in the case of $k = 8$ and $k = 16$. Data reported in Table 1b are in good agreement with crystallographic results.^{35,36} For example, the valence angles $C_1C_2C_3$ and $C_2C_3C_4$ along the chain are correctly predicted to be different, the former lower than 112° and the latter larger than 112° as it has to be in all vinyl polymers (except polyethylene), due to substituent group encumbrance. In the optimized structure the dihedral angles along the chain significantly differ from the exact value of 180° ; in fact, contrary to the case of polyethylene, now there is the lateral encumbrance of a methyl group. Similarly the helical structure and c period (6.55–6.56 Å) calculated for *i*PP are in good agreement with the corresponding experimental data ($c = 6.54$ Å).^{35,36} Also for *s*PP, the main structural parameters well reproduce the structural experimental data;³⁷ in particular, the computed period c along the chain axis is in close agreement with its experimental counterpart ($c = 5.06$ Å). The optimized structures of all polymers are shown in Figure 1.

In summary, also considering the accuracy of crystallographic data for polymers, the structure of these saturated systems containing only light atoms (C and H) is well described by a conventional DFT functional with a relatively small basis set (6-31G(d)) and number of k points.

Modeling Poly(tetrafluoroethylene) Chains. Selected geometrical parameters of different minima obtained at the PBE and PBE0 levels for perfluoroalkane oligomers of increasing lengths are compared in Tables 2 and 3, with semiempirical

results and with available experimental data. The bond lengths and the valence angles given in Tables 2 (except for C_4F_{10}) and 3 are the average values on all angles and bonds in the oligomers.

Results on perfluoroethane have been compared to the corresponding values found by Bauer et al.³⁸ by electron diffraction. Taking into account the uncertainty of the determined parameters, Table 2 seems to suggest that the PBE0 functional works better in the prediction of the structure of C_2F_6 . It has to be pointed out that Dixon et al.^{13,14} calculated the full torsion potential energy surface for the central C–C bond in C_4F_{10} ; they inferred that the global minimum is the twist-anti structure.

The results reported for the twist-anti minimum show that DFT computations are in good agreement with their Hartree–Fock counterparts; in particular the hybrid PBE0 functional gives C–F bond lengths shorter than PBE ones, and in better agreement with the computations of ref 14 and with experiments. Since it is difficult to obtain single-crystal electron diffraction data from poly(tetrafluoroethylene) and its shorter chain oligomers because of the difficulty of finding suitable solvents for growing thin microcrystals,^{39,40} most of the available structural information come from fiber X-ray diffraction data.^{6,7}

Thus to validate our results concerning perfluoro-oligomers, we resorted to crystallographic data available in the literature relative to different perfluoro-compounds containing perfluoroalkanes chains of different lengths (until $(CF_2)_8$, see Table 2). Experimental data relative to perfluoro-compounds are listed in Table 3.

It is noteworthy that the average values of C–C and C–F bond lengths in the PBE minimum energy structures are overestimated with respect to crystallographic results. On the contrary, values issuing from computations performed by the hybrid PBE0 functional are in good agreement with their experimental counterparts. However, both functionals give an average value for the CCC backbone valence angles that is smaller than experimental estimates (in this case the PBE seems to predict values which are closer to diffraction data). Similarly, the values of FCF angles are larger than measured ones.

Concerning the choice of the basis sets, the larger 6-31+G-(d,p) basis set does not seem to significantly improve results;

(35) Natta, G.; Corradini, P. *Nuovo Cimento Suppl.* **1960**, *15*, 40.

(36) Hikosaka, M.; Seto, T. *Polym. J.* **1973**, *5*, 111.

(37) Chatani, Y.; Maruyama, H.; Noguchi, K.; Asanuma, T.; Shiomura, T. *J. Polym. Sci.: Part C* **1990**, *28*, 393.

(38) Gallaher, K. L.; Yokozeki, A.; Bauer, S. H. *J. Chem. Phys.* **1974**, *78*, 2389.

(39) Smith, P.; Gardner, K. H. *Macromolecules* **1985**, *18*, 1222.

(40) Zang, W. P.; Dorset, D. L. *Macromolecules* **1990**, *23*, 4322.

Table 2. Calculated Geometrical Parameters of C₂F₆, C₄F₁₀, C₅F₁₂, C₁₀F₂₂, and C₁₆F₃₄ Optimized at Different Computational Levels^a

oligomers	computational level	d_{C-C} (Å)	d_{C-F} (Å)	FCF (deg)	FCC (deg)	CCC (deg)	θ (deg)
C ₂ F ₆	PBE/6-31G(d)	1.552	1.348	109.1	109.9		
	PBE/6-31+G(d,p)	1.564	1.351	109.0	109.9		
	PBE0/6-31G(d)	1.538	1.330	109.2	109.8		
	PBE0/6-31+G(d,p)	1.549	1.332	109.1	109.8		
	expt ³⁸	1.545	1.326	109.5	109.7		
C ₄ F ₁₀	PBE/6-31G(d)	1.558	1.361 (1.365)	109.2	108.4 (109.0)	114.4	166.4
	PBE/6-31+G(d,p)	1.570	1.366 (1.363)	108.9	109.2 (108.4)	115.2	167.9
	PBE0/6-31G(d)	1.544	1.346 (1.343)	109.3	109.2 (108.4)	114.3	166.5
	PBE0/6-31+G(d,p)	1.555	1.346 (1.344)	109.0	109.3 (108.5)	114.8	167.2
	PM3	1.598	1.346 (1.347)	105.1	110.9 (110.5)	109.4	161.1
	HF/DZP (ref 14)	1.556	1.329 (1.327)	108.6	109.5 (108.6)	114.4	164.6
C ₅ F ₁₂	PBE/6-31G(d)	1.561	1.355	108.9	109.0	114.0	163.9
	PBE/6-31+G(d,p)	1.573	1.358	108.8	108.9	114.6	163.8
	PBE0/6-31G(d)	1.547	1.338	109.1	108.9	113.8	163.7
	PBE0/6-31+G(d,p)	1.557	1.338	108.9	108.7	114.2	163.5
	PM3	1.602	1.345	106.4	110.9	109.7	162.4
C ₁₀ F ₂₂	PBE/6-31G(d)	1.565	1.358	109.2	108.7	113.51	163.0
	PBE0/6-31G(d)	1.551	1.341	109.4	108.6	113.31	162.8
	PM3	1.602	1.347	105.6	110.6	109.96	162.3
C ₁₆ F ₃₄	PBE/6-31G(d)	1.566	1.360	109.3	108.6	113.4	162.9
	PBE0/6-31G(d)	1.552	1.343	109.5	108.6	113.2	162.7
	PM3	1.602	1.347	105.6	110.6	110.0	162.3

^a The parameters relative to C₄F₁₀ are compared to those found in ref 14; bond lengths and torsion and valence angles refer to the central C–C bond and to both fluorine atoms (F and F' in Scheme 1b) linked to each carbon atom (data relative to fluorine atom F' are in brackets).

Table 3. Selected Geometrical Parameters of Different Perfluoro-Compounds Derived from Crystallographic Analysis (When Available, the Error on Last Significant Digit Is Reported in Brackets)^a

	d_{C-C} (Å)	d_{C-F} (Å)	CCC (deg)	FCF (deg)	FCC (deg)
ref 41	1.538(5)	1.335(5)	115.5(3)	108.2(3)	108.9(3)
ref 42	1.555	1.335	115.6	107.7	108.2
ref 43	1.531	1.337	115.9	107.7	108.2
ref 44	1.543(4)	1.334(4)	116.2(2)	107.2(3)	108.3(2)
ref 45	1.533	1.329	115.4	108.0	109.1

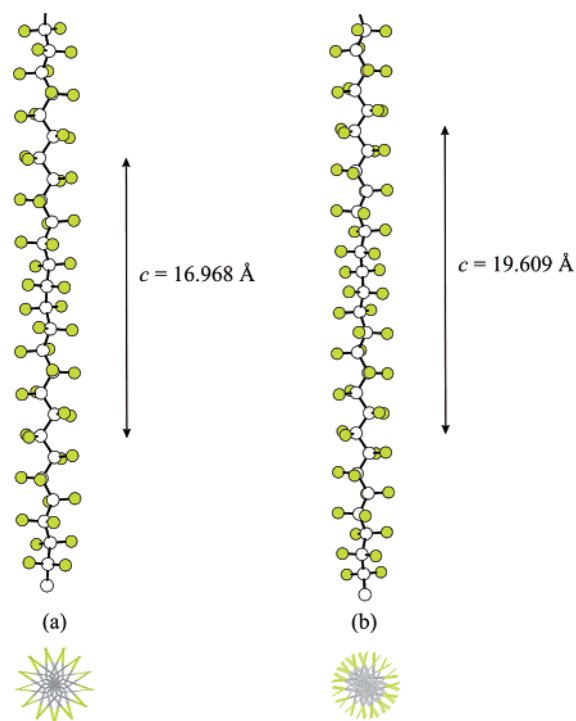
^a ref 41: [2,2,3,3,4,4,5,5-octafluorohexanedioic acid dihydrate]. ref 42: [perfluoro-1,6-bis(morpholino)hexane]. ref 43: [3-(2-(perfluorooctyl)ethoxy)nitrobenzene]. ref 44: [*trans*-2,2,3,3,4,4,5,5,6,6,7,7,8,8,9,9-hexadecafluorodecane-1,10-ditosylate]. ref 45: [1,4-dibromo-2,5-difluoro-3,6-perfluorooctylbenzene].

thus, the 6-31G(d) basis set seems adequate in describing the behavior of *n*-perfluoroalkanes.

Our ab initio calculations on long perfluoro-oligomers show that the twist in PTFE is caused by inherent electronic properties of the chain, thus confirming results found by others for the simple perfluoro-*n*-butane.^{13–15}

Next, periodic chains of the ordered helices of poly-(tetrafluoroethylene) have been considered, and the structures obtained minimizing the helices have been then analyzed.

Calculations carried out at the PBE/6-31G(d) level, predict two minima which can be classified as a 13/6 and a 15/7 helix (see Figure 2), respectively; similar results have been obtained at the PBE0/6-31G(d) level, but as we have noted in the short chain cases, the PBE0 foresees better geometries. In Figure 2 projections along the chain axis reveal a 13-pointed star (helix 13/6) and a 15-pointed star for the other helix (helix 15/7).

**Figure 2.** Regular 13/6 (a) and 15/7 (b) helices predicted at the PBE/6-31G(d)/PBC level; their projection and periods along the chain axis are also reported.

Convergence was reached in calculations carried out at the PBE/6-31G(d) and PBE0/6-31G(d) level employing 64 k points.

The main geometrical parameters (see Table 4) characterizing the two regular right-handed structures obtained by means of a PBE (PBE0) functional show an average value of $163.4^\circ \pm 0.4^\circ$

Table 4. Geometrical Parameters and Relative Stability of Predicted Periodic Right-Handed Helices

	d_{c-c} (Å)	d_{c-F} (Å)	CCC (deg)	θ (deg)	c (Å)	h (Å)
PBE						
13/6	1.568	1.362	113.2	163.4	16.968	1.305
15/7	1.569	1.362	113.3	165.7	19.609	1.307
PBE0						
13/6	1.554	1.345	113.0	163.2	16.954	1.304
15/7	1.555	1.345	113.0	165.5	19.595	1.306

^a Optimizations have been carried out at PBE/6-31G(d) and PBE0/6-31G(d) employing 64 k points on unit cells containing, respectively, 13 CF₂ and 15 CF₂ units. ^b It is noteworthy that, from an energetic point of view, DFT computations employing both PBE and PBE0 functionals indicate that the first minimum is more stable than the latter one by less than 0.1 kcal/mol of CF₂. This is in agreement with the fact that the 13/6 helix is the structure adopted by the macromolecules in the low temperature form II, whereas the 15/7 helix is the structure adopted in form IV which is stable at higher temperature.

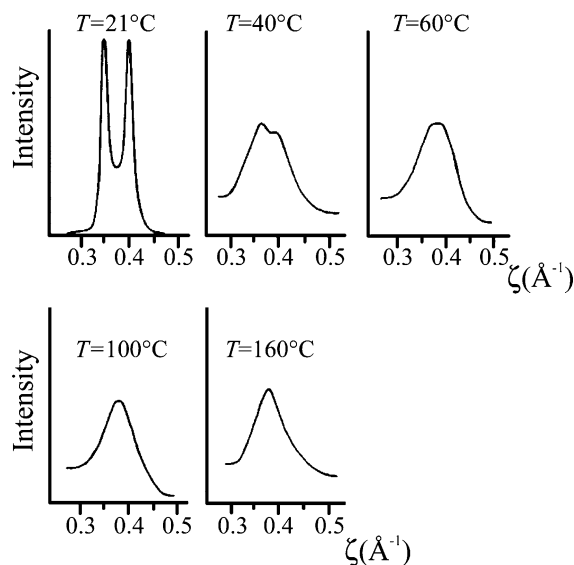


Figure 3. Experimental X-ray diffraction profiles of an uniaxially oriented PTFE sample at different temperatures redrawn from ref 11. (The value of the reciprocal coordinate ξ is fixed close to the position of intensity maximum on the seventh and eighth layer lines.)

($163.2^\circ \pm 0.3^\circ$) for the θ dihedral angles in the first minimum. This result is in good agreement with a value of 163° estimated by Clark⁴⁶ for the 13/6 helix, whereas in the latter minimum those dihedrals have an average value of $165.7^\circ \pm 0.6^\circ$ ($165.5^\circ \pm 0.5^\circ$) to be compared with a value of 166° predicted for the 15/7 helix by the same author. The computed values for the period along the chain axis are $c = 16.968 \text{ \AA}$ (16.954 \AA) and $c = 19.609 \text{ \AA}$ (19.595 \AA), respectively; thus unit heights are $h = 1.305 \text{ \AA}$ (1.305 \AA) and $h = 1.307 \text{ \AA}$ (1.306 \AA).

The good results obtained so far prompted us to use the same tools to study the phenomenon of disorder in poly(tetrafluoroethylene).

Let us consider the experimental X-ray diffraction profiles of uniaxially oriented PTFE fibers at different temperatures (see Figure 3) as a function of the reciprocal coordinate ξ .

In the profiles of Figure 3 it is apparent that while below 30°C the seventh and eighth layer lines are well defined, with increasing temperature the two layer lines become ill-defined and approach each other, merging into a single broad layer line centered in between. With a further increase in temperature (up to 160°C), the profile of the single layer line becomes progressively narrower. This behavior can be explained in terms of a thermally activated process leading to an increase of concentration of helix reversals as the temperature increases.^{10,11}

In our previous PM3 study,¹⁹ we found that, for the minimum energy conformers, the defect is always localized into a small region involving only four $-\text{CF}_2-$ units. The internal variables characterizing the junction between the two enantiomeric portions of the chain deviate only slightly from their average values in the defect-free regions. According to this analysis, these junctions may be described, on average, by sequences of the kind $\dots\text{T}^+\text{T}^+\text{T}^+ (\text{T}'^+\text{T}'^-) \text{T}^-\text{T}^-\text{T}^-\dots (\dots\text{T}^-\text{T}^-\text{T}^- (\text{T}'^-\text{T}'^+) \text{T}^+\text{T}^+\text{T}^+\dots)$ with $\text{T}^+ = -\text{T}^- = +162 \pm 2^\circ$ and $\text{T}'^+ = -\text{T}'^- = +169.8 \pm 0.3^\circ$. Two consecutive helix reversals do not interact with each other if they are separated by more than three dihedral angles and their contributions to internal energy can be considered as additive. The energy cost amounts to ~ 2.32 kcal/mol for each reversal and corresponds to an enthalpy of ~ 2.13 kcal/mol. This value is 0.6 kcal/mol higher than the corresponding value calculated by Farmer^{16,17} and also higher than the experimental estimate for the formation energy of a single helix reversal, deduced from infrared absorption intensities ($\Delta E \approx 1.25$ kcal/mol).⁸

In the study of disordered chains of perfluoro-oligomers, according to DFT, the predicted geometries for the new minima are slightly different from those obtained through PM3 calculations. In fact comparing the geometrical parameters of the models obtained in the ab initio PBE/6-31G(d) and PBE0/6-31G(d) cases with the values obtained by means of the semiempirical approach, we see that, according to the PBE functional, in nondefective right- and left-handed sequences the average values of backbone dihedral angles are $+162.6^\circ \pm 0.9^\circ$ and $-162.6^\circ \pm 0.9^\circ$, respectively, and the backbone valence angles are all nearly equal to $113.3^\circ \pm 0.5^\circ$. The corresponding values for the PBE0 functional are $+162.4^\circ \pm 0.9^\circ$, $-162.4^\circ \pm 0.9^\circ$, and $113.1^\circ \pm 0.5^\circ$ respectively.

According to PBE, the junction (see Figure 4) between two consecutive enantiomeric helical segments is characterized by a C–C–C valence angle of 114.7° , slightly wider than the average angles (113.3°) along the isochiral stems; at the same time the two dihedral angles at the reversal interface have average values of $\text{T}'^+ = -\text{T}'^- = 172.3^\circ$, i.e., $\sim 10^\circ$ wider than those in nondefective chain segments. Similar values for valence and dihedral angles characterizing junctions are obtained by the PBE0 functional, namely 114.5° and 172.2° .

Despite the fact that the geometries optimized at semiempirical and DFT levels are only slightly different, larger differences in the energetics of the reversal phenomena have been obtained. In fact, DFT calculations, with both the PBE and PBE0 functionals, estimate an energy cost for a single helix reversal of $\Delta E_r \approx 1.14$ kcal/mol against a value of $\Delta E_r \approx 2.32$ kcal/mol predicted at the PM3 level. The DFT result is not far

- (41) Centore, R.; Tuzi, A. Z. *Kristallogr. New Cryst. Struct.* **1999**, *214*, 526.
 (42) Meinert, H.; Mader, J.; Rohlf, W.; Thewalt, U.; Debaerdemaeker, T. *J. Fluorine Chem.* **1994**, *67*, 235.
 (43) Hori, K.; Kubo, C.; Takenake, S. *Mol. Cryst. Liq. Cryst. Sci. Technol., Sect. A* **2001**, *365*, 617.
 (44) De, S.; Lokanath, N. K.; Sridhar, M. A.; Shashidhara Prasad, J.; Venkatesan, K.; Bhattacharya, S. *J. Mol. Struct.* **1999**, *479*, 75.
 (45) Krebs, F. C.; Spanggaard, H. *J. Org. Chem.* **2002**, *67*, 7185.
 (46) Clark, E. S. *Polymer* **1999**, *40*, 4659.

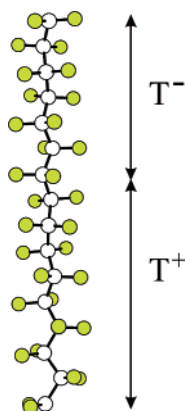


Figure 4. Detail of helix reversal along a model chain of poly(tetrafluoroethylene).

from the corresponding energy cost estimated by Farmer (1.7 kcal/mol)^{16,17} and very close to the experimental value of reversal formation energy ($\Delta E_r = 1.25$ kcal/mol)⁸ derived from infrared absorption intensities. The slightly higher experimental value can be understood considering that we are modeling a single chain, whereas the experiment refers to the three-dimensional system.

The partition function of a chain constituted by N skeletal bonds susceptible to include helix reversal defects with restraints found for our models has been obtained on the basis of the analysis concerning the reciprocal interaction of consecutive reversals along the chain. Consequently, the equilibrium concentration of defects at a given temperature and the critical temperature of coalescence of the seventh and eighth peaks have been calculated.

Also in the DFT case the defect is localized into a region involving four $-\text{CF}_2-$ units, and the interaction between two consecutive reversals is quite similar to that found in PM3 modeling. Thus we assume that sequences of dihedral angles not containing any reversal, of the kind $\dots T^\pm T^\pm T^\pm T^\pm \dots$, have energy zero; sequences containing a single helix reversal, of the kind $\dots T^\pm T^\pm (T'^\pm T'^\mp) T^\mp T^\mp \dots$, have energy equal to 1.14 kcal/mol; sequences containing two helix reversals separated by at least three bonds, of the kind $\dots T^\pm T^\pm (T'^\pm T'^\mp) (T'^\mp) (T'^\mp T'^\pm) T^\pm T^\pm \dots$ ($i \geq 1$) have energy equal to $2(1.14)$ kcal/mol. We neglect a small extra energy amount, when $n = 1$; those having three nonconsecutive helix reversals, of the kind $\dots T^\pm T^\pm (T'^\pm T'^\mp) (T'^\mp)_i (T'^\mp T'^\pm) (T'^\pm)_j (T'^\mp T'^\pm) T^\mp T^\mp \dots$, ($i, j \geq 1$), have energy equal to $3(1.14)$ kcal/mol and so on, whereas sequences having consecutive helix reversals, of the kind $\dots T^\pm T^\pm (T'^\pm T'^\mp T'^\pm) T^\pm T^\pm \dots$ or $\dots T^\pm T^\pm (T'^\pm T'^\mp) (T'^\mp T'^\pm) T^\pm T^\pm \dots$ are forbidden.

The partition function of a chain constituted by N skeletal bonds susceptible to include helix reversal defects with the above listed restraints may be calculated using the matrix formalism in ref 19, if we associate to each couple of consecutive triplet of bonds in the chain a matrix \mathbf{U} whose elements are the statistical weights of all possible states of the triplets of bonds in question with respect to all possible states of preceding triplets of bonds in the chain.¹⁹ Therefore, at a given temperature, the equilibrium concentration of helix reversal defects (D) may be calculated using the equation:⁴⁷

$$D = \frac{\partial \ln Z}{\partial \ln p} \approx \frac{\partial \ln \lambda}{\partial \ln p} \quad (4)$$

By introducing into eq 4 the critical value of D for which the two diffraction maxima on the seventh and eighth layer line merge into a single peak estimated in the calculations and the ΔH_r values reported above ($p = \exp(-\Delta H_r/RT)$), the critical temperature of coalescence has been foreseen.

We carried out the Fourier transform calculations on the model chains with different reversal frequencies obtained at the PBE0/6-31G(d) level, to compare the computed intensity to the experimental diffraction profile. These calculations suggest a coalescence of the two diffraction peaks on the seventh and eighth layer line into a single diffraction peak for models with, on average, one helix reversal every 9 CF_2 groups. Thus we have a single layer line for a critical value of helix reversal defects concentration $D \approx 1/9 = 0.117/\text{CF}_2$ units (see Figure 5).

By introducing this value of D and the estimated value of ΔH_r into eq 4, we predict that this coalescence is reached at a critical temperature of about 416 K that falls in the experimental range of temperatures $373 \text{ K} < T < 433 \text{ K}$ where the disorder phenomena occur.

As a matter of fact, the good agreement between the conformational models resulting from our calculations and experimental values shows that a high level of calculation is necessary for the complete comprehension of the studied phenomena and that the DFT employing the PBE0 functional and the 6-31G(d) basis set is already a powerful tool to treat this kind of macromolecular system and its conformational disorder.

Conclusions

The macroscopic properties of representative polymers of technological relevance in both regular and disordered forms are predicted by using first principle quantum mechanical approaches at a microscopic level.

As a first step, to validate our computational tools on polymers, polyethylene, and isotactic/syndiotactic polypropylene chains have been modeled by methods rooted in the Density Functional Theory with periodic boundary conditions (PBC). Calculations on saturated polyalkanes at the PBE/6-31G(d) level predict geometries in agreement with experimental data showing that this functional and basis set can be successfully applied to those polymers and suggesting that DFT methods employing a proper functional and basis set can be applied to more complex polymers such as poly(tetrafluoroethylene).

As a second step, calculations have been performed on shorter perfluoro-oligomers of different chain lengths employing conventional PBE and hybrid PBE0 functionals and basis sets. The results have shown that the hybrid PBE0 functional and the 6-31G(d) basis set, predicting structures in good agreement with the experimental diffraction data available in the literature for perfluoro compounds, can give an adequate description of these fluorinated systems.

As a third step, regular forms of poly(tetrafluoroethylene) have been investigated by means of DFT/PBC methods and with both conventional and hybrid functionals at the 6-31G(d) basis set level.

The optimizations result in two nearly isoenergetic minima which can be classified as 13/6 and 15/7 helices typical of forms

(47) Flory, P. J. *Statistical Mechanics of Chain Molecules*; Interscience Publishers: New York, 1969.

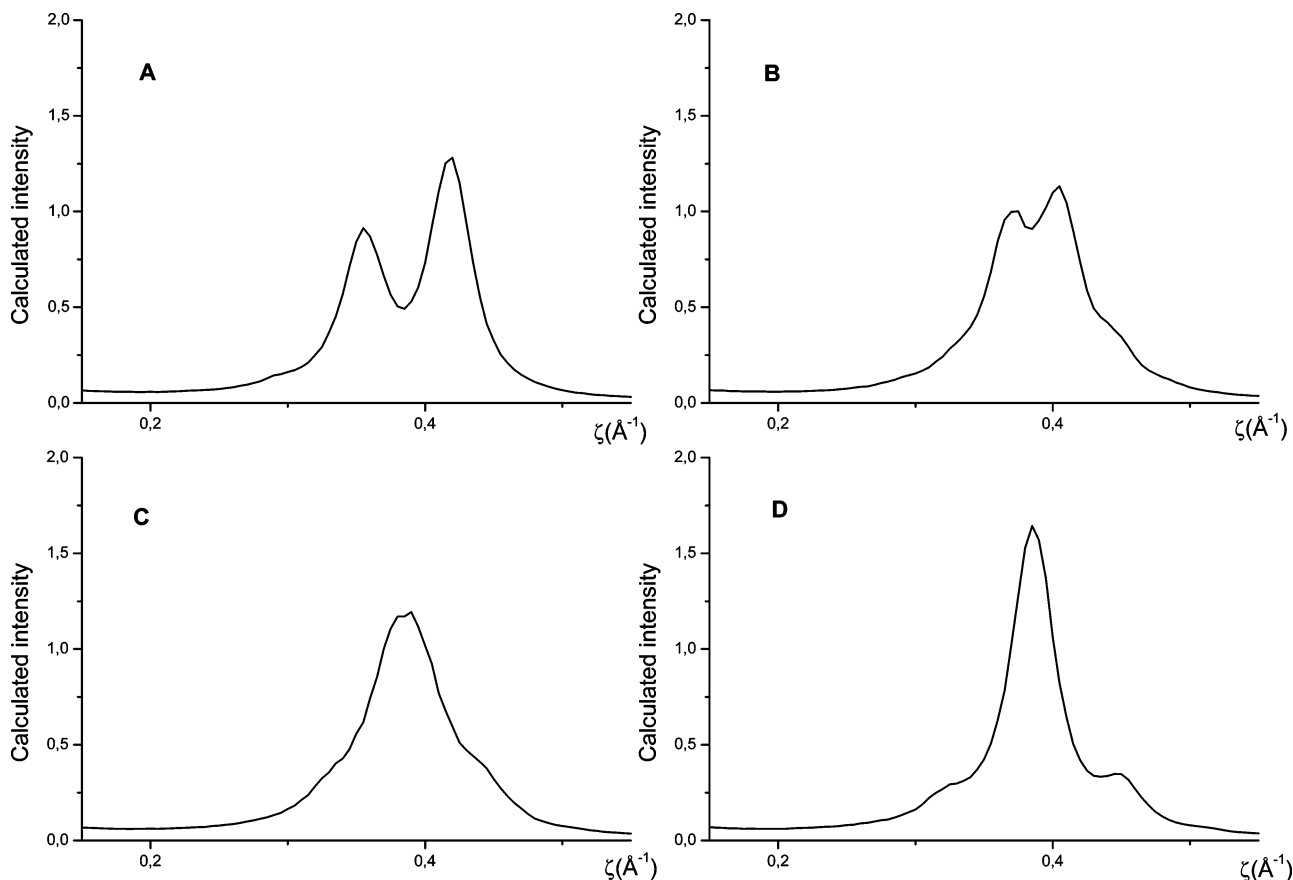


Figure 5. Calculated X-ray diffraction profiles at $\xi = 0.18 \text{ \AA}^{-1}$ for $0.15 \text{ \AA}^{-1} < \zeta < 0.55 \text{ \AA}^{-1}$ (i.e., the same region of reciprocal space as the experimental patterns of Figure 3) for model chains containing different concentrations of helix reversals. (A) No reversals; (B) 1 reversal every 10 CF_2 units; (C) 1 reversal every 9 CF_2 units; (D) 1 reversal every 7 CF_2 units.

II and IV and I, respectively. According to the PBE functional results, the model chain identifiable as the 13/6 helix presents dihedrals with an average value of $163.4^\circ \pm 0.4^\circ$ and a unit height of 1.305 \AA with a periodicity along the chain axis $c = 16.968 \text{ \AA}$; the minimum energy structure corresponding to 15/7 helix is characterized by dihedrals with an average value of $165.7^\circ \pm 0.6^\circ$ and a unit height of 1.307 \AA with a periodicity along the chain axis $c = 19.609 \text{ \AA}$. These values are in very good agreement with experimental diffraction data.

The 13/6 helix is also predicted to be more stable than the 15/7 helix, in agreement with the fact that the first is present in form II which is stable at lower temperature than the other forms (IV, I) presenting chains in 15/7 helical conformations.

Analogous results are predicted by the PBE0 functional; however as it has been found for chains of perfluoro-oligomers, this functional predicts structures whose geometrical parameters (i.e., C–C and C–F bond lengths, CCC, FCF, and FCC valence angles) are in better agreement with diffraction results reported in the literature for fluorocompounds.

Definitely, the DFT/PBC approach predicts correctly the two helical conformations of poly(tetrafluoroethylene) and their relative stabilities too, so showing that this recent computational tool is reliable in the description of polymeric systems of great technological relevance.

As a final step, disordered chains of PTFE have also been studied at the same PBE/6-31G(d) and PBE0/6-31G(d) level of calculations.

In the minima obtained for the different oligomers the defect is always localized into a small region involving only four

$-\text{CF}_2-$ units. The internal variables placed at the junction between the two enantiomorphic portions of chain deviate only slightly from their average values in the defect-free portions of chains. According to this analysis, these junctions may be described, on average, by sequences of the kind $\dots\text{T}^+\text{T}^+\text{T}^+$ ($\text{T}'^+\text{T}'^-$) $\text{T}^-\text{T}^-\text{T}^- \dots$ ($\dots\text{T}^-\text{T}^-\text{T}^-$ ($\text{T}'^-\text{T}'^+$) $\text{T}^+\text{T}^+\text{T}^+$ \dots) with $\text{T}^+ = -\text{T}'^- = +162.4 \pm 0.9^\circ$ and $\text{T}'^+ = -\text{T}'^- = 172.3^\circ$ at the PBE level, whereas the PBE0 model predicts values of $+162.2^\circ \pm 0.9^\circ$ and 172.2° , respectively. Two consecutive helix reversals do not interact with each other if they are separated by more than three dihedral angles and their contributions to internal energy can be considered additive. The energy cost for both functionals amounts to $\sim 1.14 \text{ kcal/mol}$ for each reversal.

Exploiting results obtained in our previous studies on the high temperature form of poly(tetrafluoroethylene), starting from the optimized structure of perfluoro-oligomers with 16 CF_2 units, model chains of poly(tetrafluoroethylene) with 60 CF_2 monomeric units, and a different number of reversals along the chain have been considered. Calculations of Fourier transform of minimum energy chains indicate that these models account for the experimental X-ray fiber diffraction patterns of form I of PTFE at different temperatures. Interestingly, calculations indicate that irregular conformations, not containing helix reversals, account for the presence in the diffraction patterns of broad halos on the seventh and eighth layer line and for a strong peak on the fifteenth layer line, along the meridian. By increasing the frequency of helix reversal defects, a gradual coalescence of seventh and eighth layer lines into a single

diffraction halo centered between occurs. This phenomenon, is predicted to occur for a helix reversal concentration of $\sim 1/9$ CF_2 units.

Through a statistical model, the critical concentration of defects has been related to the temperature value. The so estimated critical temperature for coalescence is of about 416 K that falls in the experimental range of temperatures $373 \text{ K} < T < 433 \text{ K}$ where the coalescence of diffuse scattering is observed in the experimental diffraction pattern.

All these results indicate that the ab initio computational strategy introduced in the present paper provides a quantitative description of the thermal behavior of disordered form I of PTFE, of the structure obtained by means of diffraction data, and of the relative stabilities of regular forms of PTFE when applied to periodic chains.

From a computational point of view, it is noteworthy that, whereas the conventional PBE functional can correctly describe saturated polyalkanes when the 6-31G(d) basis set is adopted, this functional cannot reproduce properly the behavior of electron-rich fluorocompounds. In this latter case hybrid functionals (here PBE0) are the methods of choice, whereas basis sets more extended than the polarized split valence (here 6-31G(d)) do not significantly modify the computational results.

In summary, the present paper has shown how a computational strategy based on ab initio methods rooted into DFT may be successfully applied to model polymers in both their regular and disordered forms paving the route to investigation of other complex polymers and of their disorder phenomena.

Acknowledgment. All the calculations have been performed using the advanced computer facilities of the "Campus Computational Grid"- Università di Napoli Federico II. The authors thank Gaussian Inc. and the Italian Ministry for University and Research for financial support. A special thanks is due to Prof. C. De Rosa and F. Auriemma (Università di Napoli "Federico II") for illuminating discussions and for providing us their software code which allowed us to calculate the X-ray diffraction profiles of Figure 5.

Supporting Information Available: Complete ref 27. Cartesian coordinates of the structures reported in Figure 2 and Figure 4. This material is available free of charge via the Internet at <http://pubs.acs.org>.

JA0527929